Precoder Based Transceivers Design for Non-Orthogonal Multiple Access Mixed Numerologies

Kumar P.[1,*] and Usha Rani K.R.[2]

[1] ECE Dept. Bangalore, Dayananda Sagar College of Engineering, India
[2] ECE Dept. Bangalore, R V College of Engineering, India; Email: usharani@rvce.edu.in (R.K.R.)
*Correspondence: kumarhuluvadi@gmail.com (K.P.)

***Abstract*—Orthogonal Frequency Division Multiplexing (OFDM) based mixed numerology scheme and Non-Orthogonal Multiple Access (NOMA) are the two important key features of 5G radio standard capable of handling diversified service requirements. However, the mixed numerology scheme suffers from an inherent problem called Inter Numerology Interference (INI) that arises due to non-orthogonality issue between any two numerologies, whereas NOMA suffers from potential Bit Error Rate (BER). In this research work, transmitter architecture based on windowing and pre-coding techniques to mitigate the INI and two receiver architectures based on the principle of Successive Interference Cancellation (SIC) and Combined Maximum Likelihood (CDML) decoding are proposed for optimal decoding of the information. The proposed system model is designed to operate under mixed numerology NOMA scenario. The BER performance analysis is done for both the receivers and compared with each other and the conclusive remarks are drawn.**

***Keywords*—5G, OFDM, INI, NOMA, maximum likelihood, SIC**

I. INTRODUCTION

Since the early years of 21st century, a Base Station (BS) was made to serve for a variety of wireless applications or the wireless devices in the communication world. For instance, ultra-high definition and 3D video streaming, virtual reality/augmented reality media need greater data bandwidth, while some mission critical applications such as autonomous vehicles and remote surgery demand latency as low as 1 ms. On the other hand, some low power Internet of Things (IoT) devices find their applications in smart city development are not particular about the data rate and latency, but need to work under huge connection density. These versatile applications are broadly categorized in the era of 5G into three groups, namely, *enhanced mobile broadband* (eMBB), *ultra-reliable low latency communications* (URLLC) and *massive machine type communications* (mMTC) [1, 2]. However, it was not possible for Long Term Evolution (LTE) to meet the requirements of all these heterogeneous applications, due to lack of flexibility in its spectral parameters [3–5]. Hence, Third Generation Partnership Project (3GPP) has proposed several key features, namely Orthogonal Frequency Division Multiplexing (OFDM) based multi numerologies, Non-Orthogonal Multiple Access (NOMA), massive MIMO (multiple-input and multiple-output), mm waves etc., as part of the 5G wireless standards [6]. The proposed work in this article makes an attempt to explore the benefits obtained from multi numerologies and NOMA schemes.

Multi/mixed numerologies scheme is one which allows deploying a suitable Subcarrier Spacing (SCS) among a pre-defined set, based on the requirements of an application, unless LTE which makes use of only one SCS (15 kHz) for all the applications. The flexibility of choosing a suitable predefined SCS for an application gives rise to several advantages. For instance, a latency of 1 ms can be achieved by choosing an SCS of 120 kHz for delay critical applications. This is because OFDM symbol/slot duration is inversely proportional to SCS. Also, the freedom to use higher order SCS like 120 kHz, 240 kHz helps in usage of mm wave signals (FR2: > 24 GHz) and utilize a large amount of bandwidth [7]. Though multi numerology is a promising scheme for upcoming wireless standards, system loses orthogonality when two or more numerologies are multiplexed in a single frequency band and hence a new kind of interference comes into picture called as Inter Numerology Interference (INI) [8–10].

Spectral leakage or Out of Band Radiation (OOB) is a common and major problem in single numerology OFDM based systems like LTE, that leads to deterioration of the Bit Error Rate (BER) performance at the receiver. In other words, OOB refers to one subcarrier interfering another subcarrier within an OFDM numerology. In addition to OOB, INI is another kind of interference that arises in multi numerology systems due to spectral leakage from a subcarrier of one numerology to subcarrier of another numerology [8, 9, [11]. Since, BER performance is also affected by INI, the main goal of this research work is to design the methods for mitigating INI and also design intelligent receivers to

Manuscript received September 14, 2022; revised November 30, 2022, accepted January 30, 2023.

doi:10.12720/jcm.18.7.424-434

recover the information of two users that share the same spectrum.

The first objective of this research work in addition to making use of windowing approach [12–14] is to propose a new technique called as '*precoding'* to mitigate INI [15, 16]. Precoding is a general technique which can be deployed in both single/multi users and single/multi antenna scenario for various purposes with careful design. For instance, in a MIMO system, inter user interference can be minimized in an effective way with the help of precoding if the number of users doesn't exceed the number of antennas in BS [17, 18]. A proper precoding design can improve a multiuser system in terms of both Spectral Efficiency (SE) and Energy Efficiency (EE) [19]. In single antenna system, precoding was used to localize the symbols within the symbol duration in time domain. On the other hand, in multi antenna system precoding is used to achieve spectral efficiency and energy efficiency. For example, a system with N antennas and N users works fine with precoder unless number of users doesn't exceed the number of antennas. In such a case, the BS can provide adequate degree of freedoms for the users to mitigate inter-user interference. Precoding is a technique also used for beam forming design of an antenna [3]. However, in the proposed work precoding is employed for inter numerology interference minimization.

The second objective of this research work is to explore the spectral efficiency of a Non-Orthogonal Multiple Access (NOMA) environment, consisting of diversified user services. NOMA is one such key feature in communication systems which can improve the spectral efficiency by allowing multiple users to share the spectral resources simultaneously, at the expense of some additional receiver complexity and bit error rate (BER) degradations [20]. The two well-known receiver architectures that can be used for NOMA users are Successive Interference Cancellation (SIC) receiver [21, 22] and Combined Maximum Likelihood (CDML) receiver [23].

TABLE I. ADVANTAGES OF PROPOSED WORK AS COMPARE TO EXISTING METHODS

No	Existing methods	Proposed method	Advantage of proposed method
1	Multi numerology scheme with one user per numerology [11], [15]	Multi numerology implemented in NOMA platform	Additional users can share the spectrum at the same time so spectral efficiency Improved
2	Windowing individual OFDM user [24]	Windowing applied to NOMA- multi numerology	Windowing the composite signal of two users with same cost of calculations
3	Precoding individual OFDM user [16]	Precoding applied to NOMA users.	Precoding the composite signal of two users with same cost of calculations
4	Makes use of SIC receiver so privacy is less [21]	CDML receiver is employed in NOMA multi numerology,	Increased the level of privacy.

The two major contributions of this research work are (a) employing precoding at the transmitter to mitigate INI and (b) performing and comparing BER analyses for both SIC and CDML receiver used under NOMA based mixed numerology systems. The advantages of the proposed method are listed out in the Table I.

The rest of the paper is organized as follows: In section II, proposed system model is discussed with the mathematical model details of transmitter, precoding, SIC receiver and CDML receiver. In section III, simulation results are discussed. Section IV concludes the research work carried out.

II. SYSTEM MODEL

In this section the transmitter, precoder and receivers design details are discussed.

A. *Transmitter*

The block diagram of a NOMA based downlink multi-numerology transmitter is shown in Fig. 1. In this work, the two numerologies are allowed to share the system bandwidth and two users are assigned to each numerology. Therefore, the total number of users is four. It can be noted that the transmitter architecture can be extended for multiple users per numerology and multiple numerologies. Since the power is constrained, conventionally in power domain NOMA, only two users share the power in a given numerology. Further, the analysis provided here for the case of two numerologies will also hold good for multiple numerologies. If 'B' is the system bandwidth, it will be divided into several subbands to implement suitable numerology in each subband. Since there are only two numerologies have been considered in the proposed system, two subbands of ratio p and q are assumed so that a portion of bandwidth $p\times B$ is assigned to numerology-1 (NUM-1) and the remaining portion of the bandwidth $q\times B$ is assigned to numerology-2 (NUM-2) with the subcarrier spacings of Δf_1 and Δf_2, respectively. Between the two numerologies a guard band gap of $2\Delta f_1$ is assumed.

The SCS and the symbol duration of these two numerologies are related as given in Eqs. (1, 2):

$$\Delta f_2 = 2^v \Delta f_1 \quad (1)$$

$$T_1 = 2^v T_2 \quad (2)$$

where v = 1 to 5 in the 5G communication scenarios. The simulation parameters for this work considered are as shown in Table II, with $v = 1$ and Δf_1=15 kHz.

In Fig. 1, the upper and lower branches represent numerology - 1 and numerology - 2 respectively. The two users (primary and secondary user) in a given numerology make use of the same spectral resources at any instant of time but they differ in power level while modulating the carriers in the baseband stage. Hence, the name power domain NOMA (pNOMA). The two baseband modulated signals in numerology-1 are added and passed to symbol mapper (SM) via serial to parallel converter. The SM passes the symbols to the Inverse Fast Fourier Transforms (IFFT) block. OFDM symbol is obtained by converting parallel IFFT output to serial and appending cyclic prefix (CP). Finally, windowing is done to each of the composite OFDM symbol. Similarly, the same principle holds good for numerology-2 except for the precoding process in which a certain number of symbols of parallel symbol mapper are precoded before they are passed to IFFT block as shown in Fig. 1.

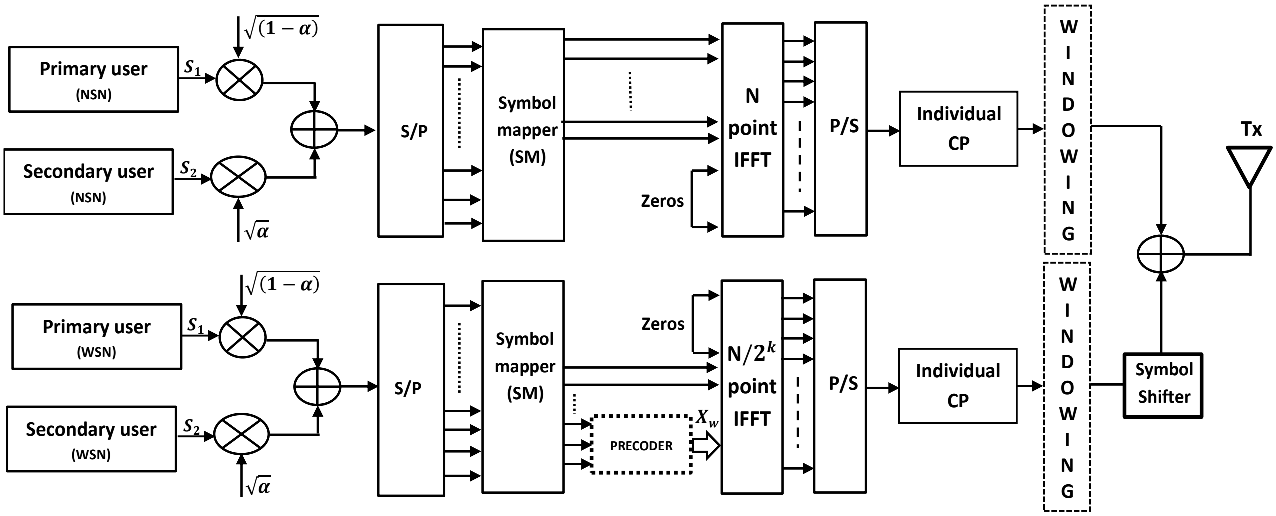

Figure 1. Block diagram of NOMA based downlink multi-numerology transmitter [11,[15].

TABLE II. SIMULATION PARAMETERS OF NUMEROLOGY-1 & NUMEROLOGY -2 [25]

Parameters	Numerology-1 (NSN)	Numerology-2 (WSN)
Subcarrier spacing (kHz)	15	30
OFDM Symbol Duration (μs)	66.67	33.33
CP Duration (μs)	4.69	2.34
Slot Duration (*ms*)	1	0.5
FFT size	256	128
Baseband Modulation	QPSK / 4-QAM	QPSK / 4-QAM
Number of users	2	2

The proposed model is based on multicarrier modulation technique and the subcarriers in a given numerology are orthogonal to each other. However, pair of subcarriers coming from different numerologies are not orthogonal to each other as their SCS are different. Therefore, after multiplexing the data at the transmitter, the non-orthogonality issue between the numerologies leads to interference from one numerology to the other. One way to retain the system orthogonality is to use a single numerology in the whole spectrum but it is not useful for multiplexing a variety of services. Since it is desired to multiplex as many users as possible in URLLC, the proposed work exploits the concept of pNOMA and analyzes the impact of INI on the secondary users.

To minimize the INI, output of each numerology is windowed using a window function as shown in Fig. 1. The composite signal at the output of the transmitter is given by Eq. (3) as:

$$y(t) = w_1 x^{NSN}(t) + w_2 x^{WSN}(t) \tag{3}$$

Here, we use the alternate terms NSN (Narrow Subcarrier Spacing) and WSN (Wide Subcarrier Spacing) for numerology-1 and numerology-2 respectively for convenience. The terms $x^{NSN}(t)$ and $x^{WSN}(t)$ represent the time domain output of numerology-1 (NSN) and numerology-2 (WSN) respectively and w_1 and w_2 are the window functions used for numerology-1 and numerology-2 respectively.

B. Precoding

Precoding is a kind of encoding the baseband symbols in some way, before they modulate the subcarriers so that the modulated subcarriers result in least interference to the subcarriers of the adjacent numerologies [26]. Logically the base band symbols are multiplied with precoder matrix *G* before OFDM modulation as shown in Fig. 1. The algorithm used to design a precoder matrix is as follows:

Step 1: Initialize orthonormal matrix $\tilde{G}$ of dimension $(N_2 \times N_2)$ with random phases. Here, N_2 represents the number of subcarriers in numerology 2 and *M* represents the number of subcarriers causing INI.

Step 2: Obtain

$$\tilde{G}X_1 = \bar{X}_1 \tag{4}$$

Step 3: If last *M* values of $\bar{X}_1$ are zero, then, compute

$$A = \left(G^H G + \alpha I_{N_2}\right)^{-1} \tag{5}$$

where I_{N_2} is an identity matrix of size $(N_2 \times N_2)$ and α called regularization factor taken as 0.1

Step 4: If

$$\left\|A\tilde{G}\bar{X}_1 - X_1\right\|^2 < \epsilon \tag{6}$$

Then stop and exit, else go to **step 2** to update $\tilde{G}$. If all conditions are met stop and exit.

C. Receiver

The two receiver architectures discussed in this section are the SIC receiver & the CDML receiver whose block diagrams are shown in Fig. 2 and Fig. 3 respectively. In both SIC and CDML receivers, the primary user is demodulated on the principle of ML, but the difference comes in the secondary user demodulation. The secondary user of SIC receiver is demodulated on the principle of SIC while that of CDML receiver is demodulated on the principle of CDML. The received composite signal $y_c(t)$ is given by Eq. (7) as:

$$y_c(t) = w_1 x^{NSN}(t) \circledast h^{NSN}(t) + w_2 x^{WSN}(t) \circledast h^{WSN}(t) \quad (7)$$

where $h^{\mathrm{NSN}}(t)$ and $h^{\mathrm{WSN}}(t)$ are the impulse responses of the flat fading channel. For simplicity assuming:

$$h^{NSN}(t) = h^{WSN}(t) = h(t) \quad (8)$$

Using Eq. (8) in Eq. (7), it gives:

$$y_c(t) = [(w_1 x^{NSN}(t) + w_2 x^{WSN}(t)] \circledast h(t) \quad (9)$$

After sampling $y_c(t)$ at the receiver using the Nyquist Sampling $t = nT_s$, the output of ADC is given by Eq. (10) as:

$$y_c(n) = w_1 x^{NSN}(n) \circledast h^{NSN}(n) + w_2 x^{WSN}(n) \circledast h^{WSN}(n) \quad (10)$$

with

$$x^{NSN}(n) = \sqrt{(1-\alpha)}\, s_1^{NSN}(n) + \sqrt{\alpha}\, s_2^{NSN}(n) \quad (11)$$

and

$$x^{WSN}(n) = \sqrt{(1-\alpha)}\, s_1^{WSN}(n) + \sqrt{\alpha}\, s_2^{WSN}(n) \quad (12)$$

where s_i is the symbol of the i^{th} user. The discrete windowing functions w_1, and w_2 are given by the Eqs. (13, 14) as

$$w_1(n) = \frac{1}{\sqrt{N_{sc_1}}} g(n - N_T) \quad (13)$$

$$w_2(n) = \frac{1}{\sqrt{N_{sc_2}}} g(n - N_T) \quad (14)$$

where N_{sc_1}, N_{sc_2} are the scaling factors. Applying N-point DFT/FFT to Eq. (10) with length based on the corresponding numerology, the frequency domain expression of the received signal is given by Eq. (15) as

$$Y_c(k) = \sum_{n=0}^{N-1} y_c(n) e^{-\frac{j2\pi nk}{N}}, \ k = 0, 1 \ldots\ldots, N-1 \quad (15)$$

Alternatively, Eq. (15) can be written as:

$$Y_c(k) = \left(W_1 X^{NSN}(k) H^{NSN}(k) + W_2 X^{WSN}(k) H^{WSN}(k) \right) \quad (16)$$

$$Y_c(k) = Y_{NSN}(k) + Y_{WSN}(k) \quad (17)$$

where,

$$Y_{NSN}(k) = W_1 X^{NSN}(k) H^{NSN}(k) \quad (18)$$

and

$$Y_{WSN}(k) = W_2 X^{WSN}(k) H^{WSN}(k) \quad (19)$$

where $X^{NSN}(k)$ and $X^{WSN}(k)$ are the frequency domain signal of $x^{NSN}(n)$ and $x^{WSN}(n)$ obtained using DFT equation as shown below in Eqs. (20, 21) as:

$$X^{NSN}(k) = \sum_{n=0}^{N-1} x^{NSN}(n) e^{-\frac{j2\pi nk}{N}}, \quad k = 0,1, \ldots (N-1) \quad (20)$$

$$X^{WSN}(k) = \sum_{n=0}^{M-1} x^{WSN}(n) e^{-\frac{j2\pi nk}{M}}, \quad k = 0,1, \ldots (M-1) \quad (21)$$

Alternatively, $X^{NSN}(k)$ and $X^{WSN}(k)$ are obtained by taking DFT for Eqs. (11, 12) as follows:

$$X^{NSN}(k) = \sqrt{(1-\alpha)}\, S_1^{NSN}(k) + \sqrt{\alpha}\, S_2^{NSN}(k) \quad (22)$$

$$X^{WSN}(k) = \sqrt{(1-\alpha)}\, S_1^{WSN}(k) + \sqrt{\alpha}\, S_2^{WSN}(k) \quad (23)$$

Successive Interference Cancellation Based Receiver: This section deals with the successive interference cancellation-based receiver design. In the SIC receiver, there are two stages, the output of first stage is the estimate of $S_1^{NSN}(k)$ represented as $\hat{S}_1^{NSN}(k)$, and obtained using Maximum Likelihood (ML) equation given by the Eq. (24) as:

$$\hat{S}_1^{NSN}(k) = \underset{C_1}{argmin} \left\| \frac{Y_{NSN}(k)}{\sqrt{(1+\alpha)}} - C_1 \right\|^2, \quad k = 0,1, \ldots, (N-1) \quad (24)$$

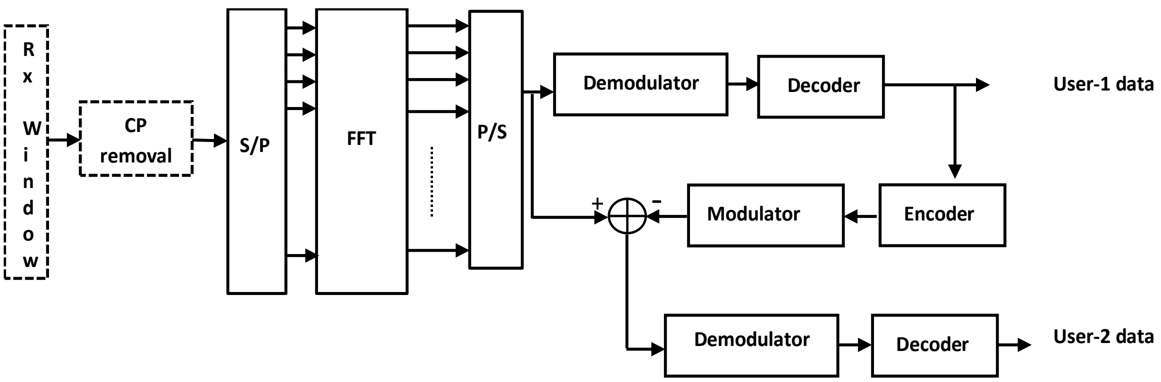

Figure 2. Block diagram of NOMA based downlink multi-numerology receiver based on SIC.

In the above Eq. (24), $\|.\|$ is the Frobenius norm. The Frobenius norm of a vector $A = \{a_1, a_2, \dots a_N\}$ is calculated as:

$$\|A\| = \sqrt{\sum_{i=0}^{N} |a_i|^2} \quad (25)$$

For each k value, the symbol $\hat{S}_1^{NSN}(k)$ also denoted as $\widehat{X_1}(k)$ is thus obtained by computing Frobenius norm over each C_1 and selecting the constellation that results in minimum distance. Here C_1 is the complex symbol obtained from M-QAM constellation used at numerology −1 primary user. For instance, with:

$$M = 4,\ C_1 \in [c_{11},\ c_{12},\ c_{13},\ c_{14}] \quad (26)$$

$$M = [0.707 + 0.707i,\ -0.707 + 0.707i,\ -0.707 - 0.707i,\ 0.707 - 0.707i] \quad (27)$$

Once $\hat{S}_1^{NSN}(k)$ is obtained, the estimate of $\hat{S}_2^{NSN}(k)$ is obtained as follows. According to the principle of SIC an intermediate symbol $\widehat{Y_2}(k)$ is calculated using the Eq. (28) as:

$$\widehat{Y_2}(k) = Y_{NSN}(k)\sqrt{(1+\alpha)} - \frac{1}{\sqrt{\alpha}}\widehat{X_1}(k) \quad (28)$$

Finally, the required estimate of $\hat{S}_2^{NSN}(k)$ is computed using the Eq. (29) as:

$$\hat{S}_2^{NSN}(k) = \underset{C_2}{argmin}\ \|Y_2(k) - C_2\|^2, \quad k = 0,1,\dots,(N-1) \quad (29)$$

Here, C_2 is the complex symbol obtained from M-QAM constellation used at numerology -1 secondary user. Similarly, after applying M -point FFT at the WSN receiver, the estimated symbols of numberlog-2 (WSN) receiver are given by:

$$\hat{S}_1^{WSN}(k) = \underset{C_1}{argmin}\ \left\|\frac{Y_{WSN}(k)}{\sqrt{(1+\alpha)}} - C_1\right\|^2, k = 0,1,\dots,(M-1) \quad (30)$$

$$\hat{S}_2^{WSN}(k) = \underset{C_1}{argmin}\ \|Y_2(k) - C_2\|^2, k = 0,1,\dots,(M-1) \quad (31)$$

Usually in power domain NOMA, only two users are entertained; because it is difficult to differentiate more than two users in terms of power level alone. Moreover, the receiver complexity increases at all the NOMA users. Hence the numbers of power domain NOMA users are limited to two. On the other hand, 4-QAM is used in the proposed work and still it is possible to provide the closed form solution to the receiver estimators (Eqs. 24, 29–31) by going with M-ary QAM (M = 8, 16,….) to increase the bandwidth efficiency but denser points in the constellation leads increased error rates [26–28]. Thus, maximum of two pNOMA users each with 4-QAM are said to be suitable for optimal performance.

Combined Maximum Likelihood Based Receiver (CDML Receiver): In this section, the CDML based receiver design is presented in a nutshell. Similar to SIC receiver, in the combined ML receiver the output of primary user is estimated using ML over primary user constellation. The ML equation is given by the Eq. (32) as:

$$\hat{S}_1^{NSN}(k) = \underset{C_1}{argmin}\ \left\|\frac{Y_{NSN}(k)}{\sqrt{(1+\alpha)}} - C_1\right\|^2, \quad k = 0,1,\dots,(N-1) \quad (32)$$

For each k value, $\widehat{X_1}(k)$ is thus obtained by computing Frobenius Norm over each C_1 and selecting the constellation that results in minimum distance (referring to Fig. 7). The output of secondary user is obtained using the following combined Maximum Likelihood equation as given by the Eq. (33):

$$\{\hat{S}_1^{NSN}(k), \hat{S}_2^{NSN}(k)\} = \left\|Y_{NSN}(k)\sqrt{(1+\alpha)} - C_1 \odot C_2\right\|^2, \quad k = 0,1,\dots,(M-1) \quad (33)$$

In the above Eq. (33), $C_1 \odot C_2$ is the Hadamard product of vectors C_1 and C_2. For vectors $C_1 = \{c_{11}, c_{12}, \dots c_{1u}\}^T$ and $C_2 = \{c_{21}, c_{22}, \dots, c_{2v}\}^T$, the Hadamard product is given by the Eq. (34) as:

$$\begin{bmatrix} c_{11} \\ c_{12} \\ \vdots \\ c_{1u} \end{bmatrix} \circ \begin{bmatrix} c_{21} \\ c_{22} \\ \vdots \\ c_{2v} \end{bmatrix} = \begin{bmatrix} c_{11}c_{21} & c_{11}c_{22} & \cdots & c_{11}c_{2v} \\ c_{12}c_{21} & c_{12}c_{22} & \cdots & c_{12}c_{2v} \\ \vdots & \vdots & \cdots & \vdots \\ c_{1u}c_{21} & c_{1u}c_{22} & \cdots & c_{1u}c_{2v} \end{bmatrix} \quad (34)$$

Since C_1 and C_2 are QAM constellations, the Hadamard product result in combined constellation. An example constellation is given below in Fig 6. Similarly, for the WSN receiver, the estimated symbols are given by the Eq. (35) as:

$$\hat{S}_1^{WSN}(k) = \underset{C_1}{argmin}\ \left\|\frac{Y_{WSN}(k)}{\sqrt{(1+\alpha)}} - C_1\right\|^2, \quad k = 0,1,\dots,(M-1) \quad (35)$$

For each k value, $\widehat{X_1}(k)$ is thus obtained by computing Frobenius norm over each C_1 and selecting the constellation that results in minimum distance. The output of secondary user is obtained using the following combined ML equation given by Eq. (36) as:

$$\{\hat{S}_1^{WSN}(k), \hat{S}_2^{WSN}(k)\} = \left\|Y_{WSN}(k)\sqrt{(1+\alpha)} - C_1 \odot C_2\right\|^2, \quad k = 0,1,\dots,(M-1) \quad (36)$$

This work considers a downlink power-domain NOMA system that supports two simultaneous users, user-1 and user-2. All User Equipment (UE) and the BS are equipped with a single antenna and the data for user-1 and user-2 are modulated using square QAM with the same modulation order 4. It is assumed that all the symbols are equally probable. The constellation for user-1 and user-2 are shown in Figs. 4, 5 respectively.

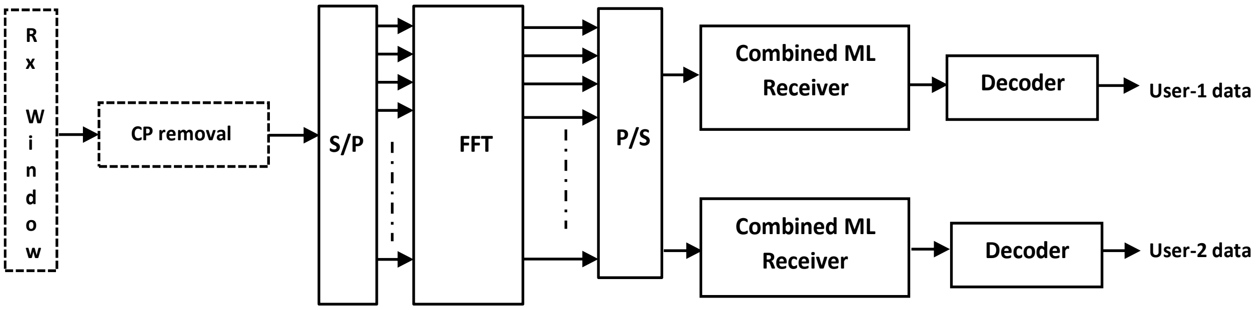

Figure 3. Block-diagram of the CDML receiver.

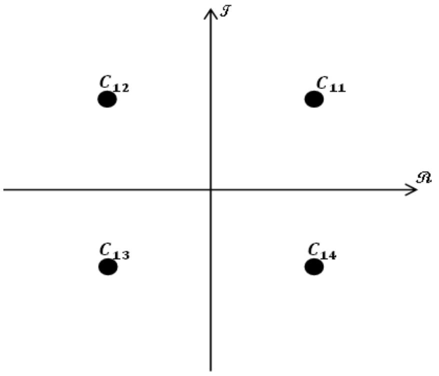

Figure 4. User-1 constellation diagram.

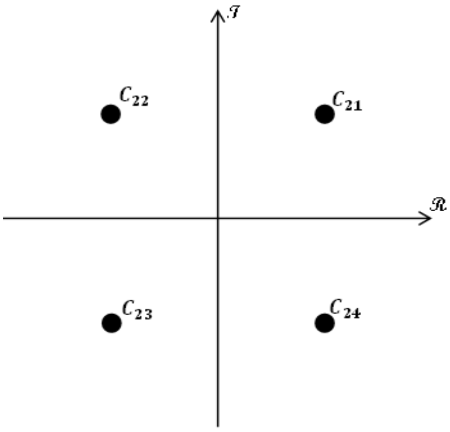

Figure 5. User-2 constellation diagram.

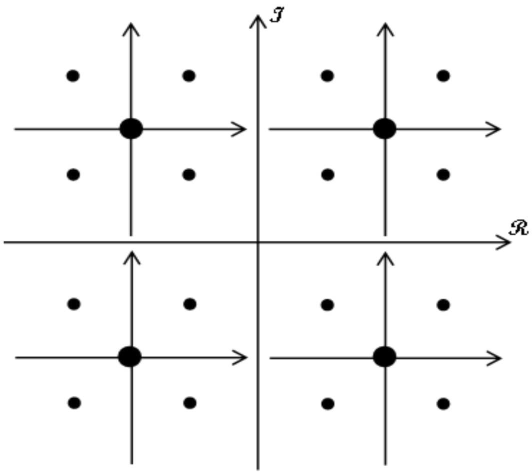

Figure 6. Super/combined constellation for user 2 maximum likelihood [22].

The user-1 demodulates its data independently using the constellation shown in Fig. 7 as follows. The distances R_{11}, R_{12}, R_{13} and R_{14} are calculated and the one which is least among them corresponds the received symbol. But user-2 demodulation process depends on the user-1 symbol that has been transmitted. In other words, the distances R_{21}, R_{22}, R_{23}, and R_{24} to be calculated depending on the quadrant the combined symbol falls into.

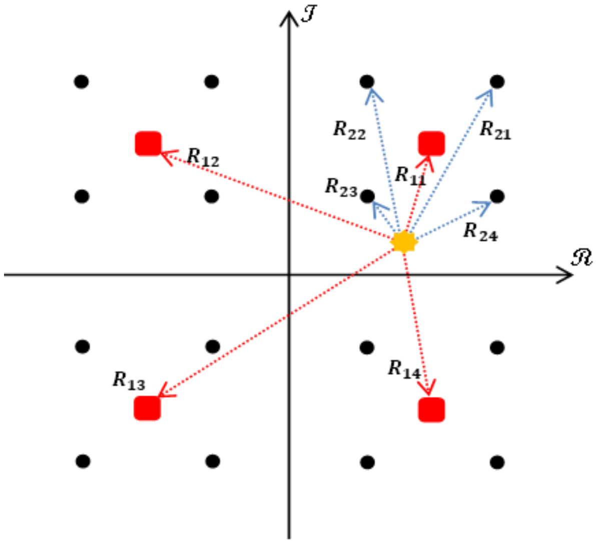

Figure 7. Super/combined constellation for user 2 ML with distances indicated [22].

III. Result and Discussion

In this section, we obtain the simulation results in terms of BER curves for both SIC and CDML receivers by considering an important parameter that affects INI, namely the power offset. Here, we define two different power offset terms namely power offset between the numerologies denoted as '*num_power_offset*' and the power offset between the primary and secondary user of a given numerology, denoted as '*user_power_offset'*.

In the system described in this work, the transmitted power is shared between the two numerologies while the power allocated to a given numerology will be shared between the primary and secondary users under that numerology. It should be noted that a user in the system discussed is denoted as *user-ij*. Here, $i = 1, 2$ indicates numerology number and $j = 1, 2$ refers to primary and secondary users respectively.

In the simulation results, it should be noted that INI expressed in dB represents the power offset between the numerologies. In all the simulation results numerology-1 is kept relatively at high power level as compared to that of numerology-2 except for 0 dB INI which refers to equal power share between the numerologies. Also, in this work the main focus of analysis is more towards the primary users of both the numerologies. Hence, they kept at relatively higher power levels as compared to that of secondary users. The BER performance simulation results are shown for both SIC and CDML receivers for various values of '*user_power_offset*'.

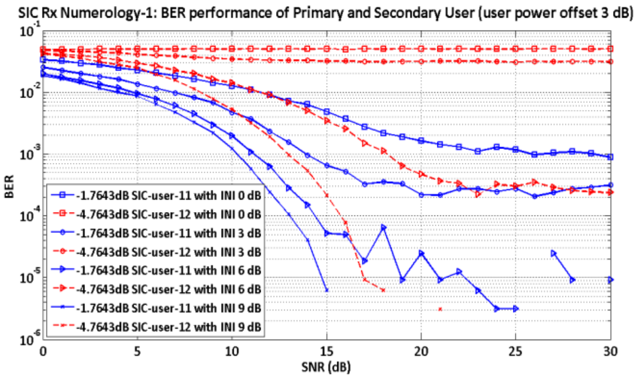

Figure 8. SIC Receiver numeroloy-1 BER performance of the primary user & secondary user (user power offset 3 dB).

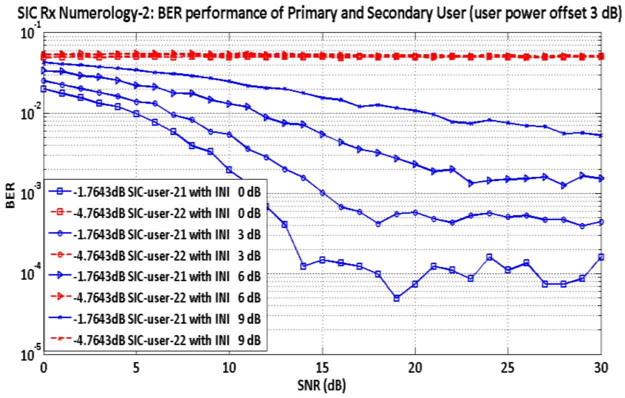

Figure 9. SIC Receiver numeroloy-2 BER performance of the primary user & secondary user (user power offset 3 dB).

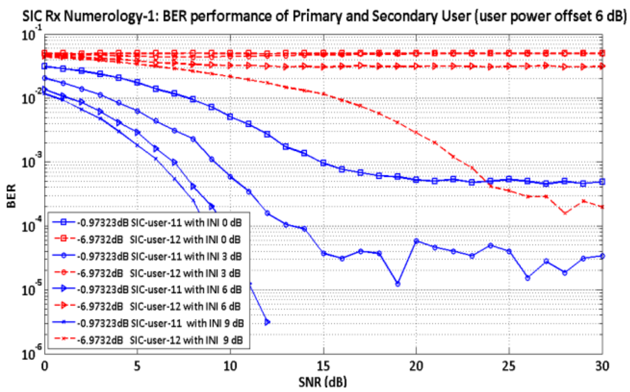

Figure 10. SIC receiver numerology-1 BER perfromance of primary user & secondary user (user power offset of 6 dB).

The 0 dB INI in the simulation results refers to equal power share between the numerology-1 and numerology-2. Since the numerology with relatively smaller SCS do suffer more from INI, i.e., numerology-1 primary and secondary users experience greater error rate as compared to that of numerology-2. This can be observed in SIC receiver by comparing the Figs. 8, 9 or Figs. 10, 11. On the other hand, same behavior can also be observed in CDML receiver by comparing the CDML results as shown in the Figs. 12, 13 or Figs. 14, 15.

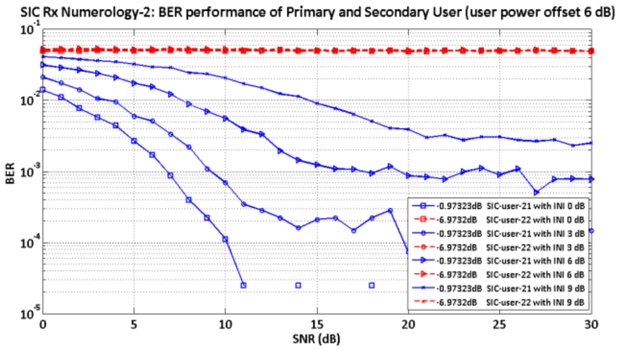

Figure 11. SIC receiver numerology 2 BER performance of primary user & secondary user (user power offset of 6 dB).

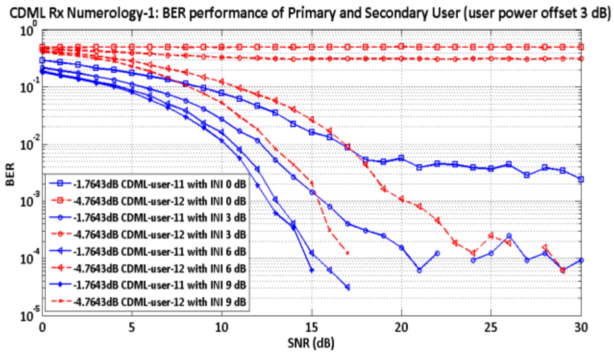

Figure 12. CDML reciever numerology 1 BER performance of primary user & secondary user (user power offset of 3 dB).

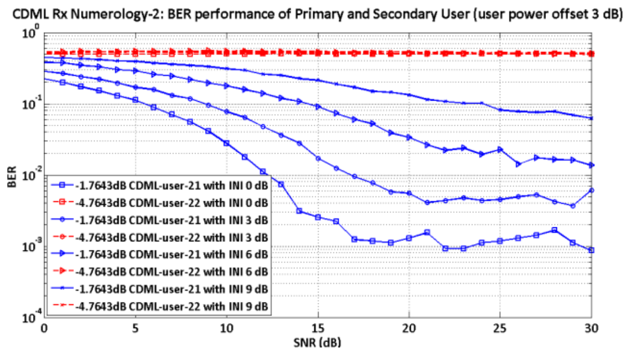

Figure 13. CDML receiver numerology 2 BER performance of primary user and secondary user (user power offset of 3 dB).

For a given value of user_power_offset, as the num_power_offset is increased (through 0 dB, 3 dB, 6 dB and 9 dB), INI experienced by numerology-1 reduces as it is kept relatively at higher power levels and hence both of its users' (primary and secondary) BER performance will be improved, whereas, INI experienced by numerology 2 increases as it is relatively at lower power level and hence both of its users' (primary and secondary) BER performances will get degraded. This behavior can be seen in both SIC receiver (Figs. 8, 9 for numerology-1 and Figs. 10, 11 for numerology-2) and CDML receiver (Figs. 12, 13 for numerology-1 and Figs. 14, 15 for numerology-2).

For a given value of num_power_offset as the user_power_offset is increased (from 3 dB to 6 dB) the performance of the primary user improves while it degrades for secondary users. This is because increase in user_power_offset pushes the primary users to relatively high-power level as compared to that of secondary users. This phenomenon can be seen for SIC receiver in both numerology-1 (compare Figs. 8, 9) and numerology-2 (compare Figs. 10, 11). This phenomenon is also observed in CDML receiver under numerology-1 (compare Figs. 12, 13) and numerology-2 (compare Figs. 14, 15).

Now the overall comparison of the BER performance of SIC and CDML receiver is shown in Figs. 16 and 17 for numerology-1 and numerology-2 respectively. It is observed that the SIC receiver out performs the CDML receiver. But, this not always the case as the performance also depends on the channel condition as well. In the work carried out here AWGN channel is assumed. However, there is a trade-off between the two. Though CDML receiver under performs it is better in terms of privacy as compared to SIC receiver. Finally, the effect of precoding of a numerology on itself and the adjacent numerology is demonstrated in the Figs. 18, 19 for CDML receiver.

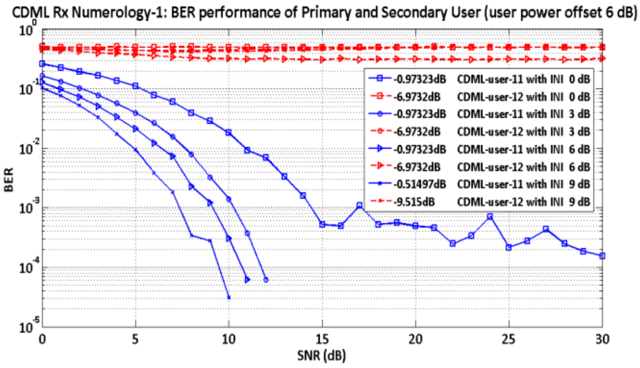

Figure 14. CDML receiver numereology 1 BER performance of primary user and secondary user (user power offset of 6 dB).

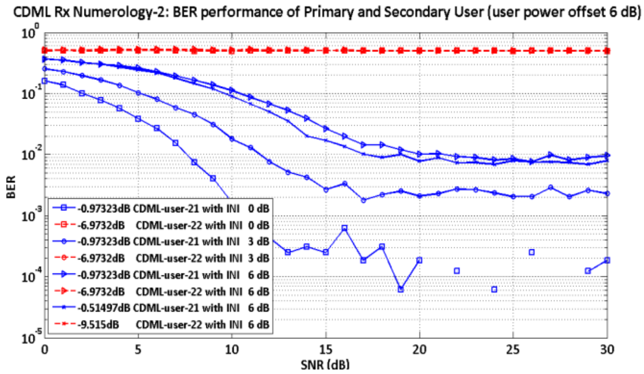

Figure 15. CDML receiver numerology 2 BER performance of primary user and secondary user (user power offset of 6 dB).

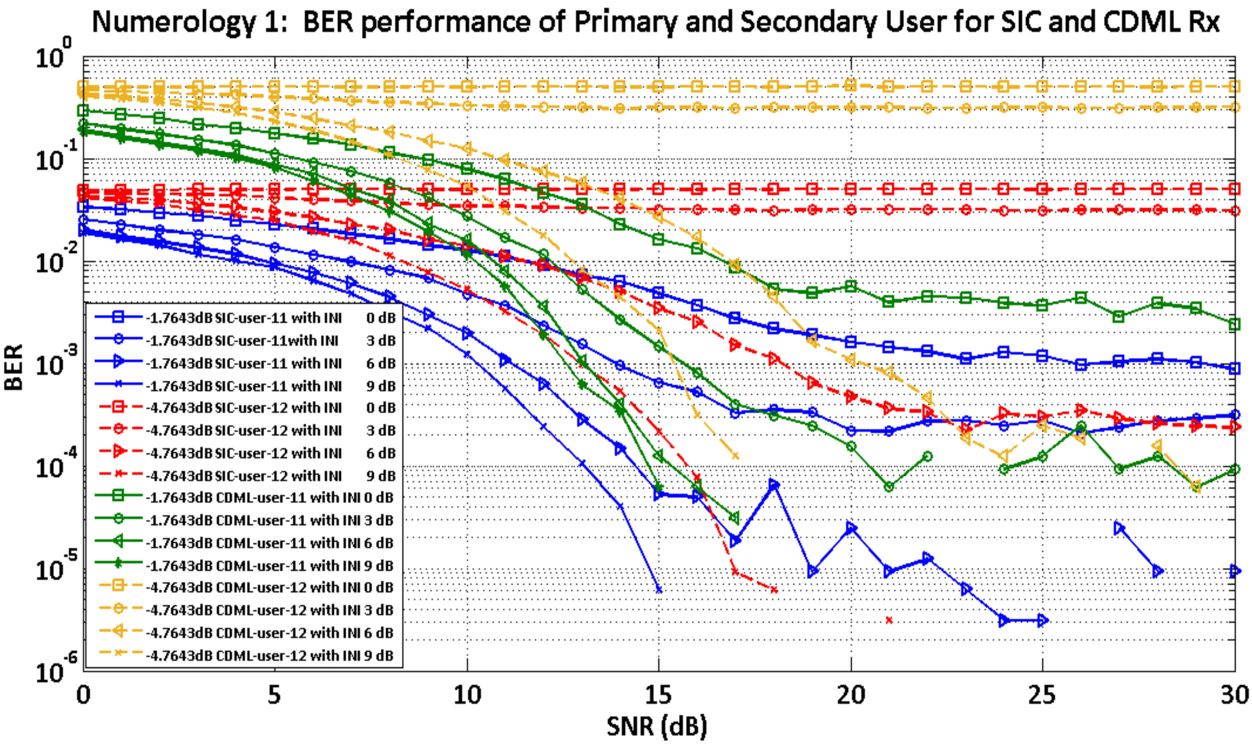

Figure 16. BER performance comparison of SIC and CDML receiver for numerology-1.

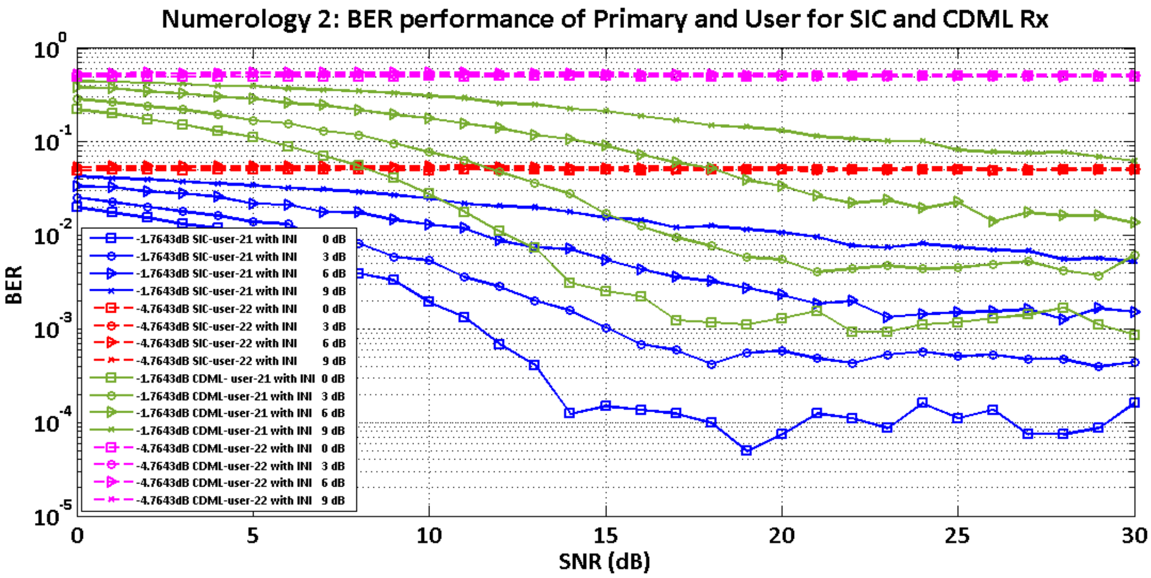

Figure 17. BER performance comparison of SIC and CDML receiver for numerology-2.

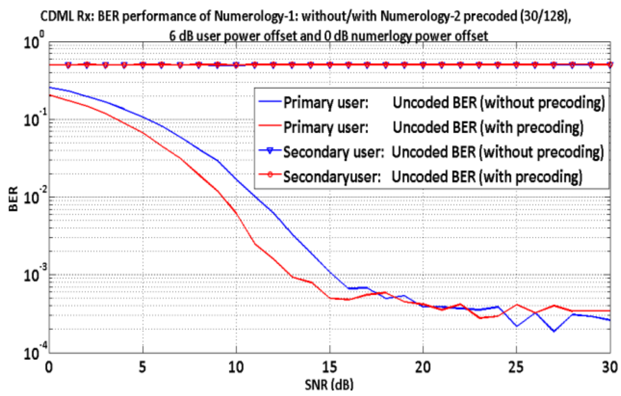

Figure 18. CDML Rx – BER performance of numerology-1 without / with numerology-2 pre-coded (30/128), 6 dB user power offset and 0 dB numerology power offset.

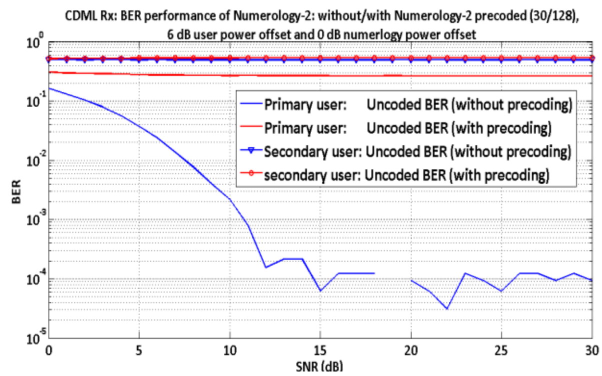

Figure 19. CDML Rx – BER performance of numerology-2 without / with numerology-2 pre-coded (30/128), 6 dB user power offset and 0 dB numerology power offset.

Channel coding is an important technique in communication systems for overcoming the errors introduced in the channel, but in order for highlighting the role of precoding technique in minimizing the errors, uncoded (without channel coding) data transmission is considered. Here, numerology-2 is pre-coded thereby numerology-1 got benefited in terms of BER performance while it got worse for numerology-2 as it is clear from the BER curves shown in the Fig. 18 and Fig 19 for the two numerologies.

A. Complexity Analysis

Conventionally, computational complexity is dominated by the number of complex multiplications required as compared to that of additions. This is because adder is easier to implement compared to multiplier. Hence the number of complex multiplications required at each user and for each receiver quantified in Table III by referring to Eqs. (7–9) and Eqs. (12, 13). Since each complex multiplication is equivalent to 4 real multiplications, the factor 4 is involved in all the terms of Table III. And, it is multiplied by N or M as there are N or M number of subcarriers. Also, at each subcarrier there are M_q^p / M_q^s number of possible constellation symbols. Hence overall computational complexity of primary user is 4NM_q^p/4NM_q^s. At the secondary user, the SIC receive will result in same number of multiplications as compared to primary user. However, the combined ML will result in more multiplications due to the combined Constellation or overall constellation. However, unlike the case of combined ML receiver, it can be noted that in SIC, the complexity of the receiver is significant due to the re-encoding and re-modulating the decoded primary symbols, as evident in block diagram shown in Fig. 2.

TABLE III. NUMBER OF COMPLEX MULTIPLICATIONS IN VARIOUS USERS

Receiver	NSN		WSN	
	Primary User	Secondary User	Primary User	Secondary User
SIC	$4NM_q^p$	$4NM_q^p$	$4NM_q^p$	$4NM_q^p$
Combined ML	$4NM_q^p$	$4NM_q^p\ M_q^s$	$4NM_q^p$	$4NM_q^p\ M_q^s$

IV. Conclusion

In this paper the role of precoder in mitigating INI is investigated and two efficient receivers are discussed for mixed numerology NOMA scenarios. The simulation results are obtained on MATLAB environment. It is observed from the simulation results that, the BER performances of all the four users in the system are dependent on the parameters like '*num_power_offset*' and '*user_power_offset*', and the number of subcarriers under its corresponding numerology. The overall performance of numerology-1 was found to be better as compared to that of numerology-2 because of the two important observations. Firstly, the number of subcarriers in numerology-1 was taken to be double that of numerology-2. Secondly, numerology-1 is allocated with higher power levels compared to numerology-2. For instance, the primary user under numerology-1 performed better as its power level and its numerology power level were found to be high. On the other hand, the secondary user under numerology-2 performed poorly as its power level and numerology power levels were found to be the least. These two constraints were well explored in this research work under the NOMA scenario, which is clearly noticed from the simulation results.

However, the performance of intended user can be brought to the required level through several ways, which can be thought of as future works. For instance, adjusting the transmitted signal power of intended user and all the other users, implementing windowing and precoding in the interfering numerology etc., could be taken up in this context. Another insight of this research work is that, a trade-off is observed between the SIC and CDML receivers in terms of BER, security and complexity. Further, it is also observed that the SIC receiver outperformed the CDML receiver, but CDML receiver was extremely good in terms of security aspects and was found to be less complex as compared to former one.

Conflict of Interest

The submitted work was not subjected to any conflict of interest. Further the authors declare "no conflict of interest".

Author Contributions

Kumar P. took responsibility of mathematical modeling and implementation, while the author Usha Rani K. R. helped in reviewing and correcting the simulation results and also documentation. all authors had approved the final version.

References

[1] 3rd Generation Partnership Project (3GPP), "Study on scenarios and requirements for next generation access technologies, Release 14," *Technical Specification*, vol. 38, p. 913, ver 14.3.0, Aug. 2017.

[2] J. G. Andrews *et al*., "What will 5G be?" *IEEE Journal on selected Areas in Communications*, vol. 32, no. 6, pp. 1065–1082, 2014.

[3] F. Alessio *et al.*, "RIS-aided joint localization and synchronization with a single-antenna receiver: Beamforming design and low-complexity estimation," *IEEE Journal of Selected Topics in Signal Processing*, 2022.

[4] A. Fascista, A. Coluccia, H. Wymeersch *et al.*, "Downlink single-snapshot localization and mapping with a single-antenna receiver," *IEEE Transactions on Wireless Communications*, vol. 20, no. 7, pp. 4672–4684, July 2021

[5] T. X. Vu, S. Chatzinotas, and B. Ottersten, "Dynamic bandwidth allocation and precoding design for highly-loaded multiuser MISO in beyond 5G networks," *IEEE Transactions on Wireless Communications*, vol. 21, no. 3, pp. 1794–1805, March 2022.

[6] S. Fiji and S. Tabbane, *5G networks and 3GPP Release 15*, Consultado, 2019.

[7] F. W. Vook *et al.*, "5g new radio: Overview and performance," in *Proc. 2018 52nd Asilomar Conference on Signals, Systems, and Computers*, IEEE, 2018.

[8] A. A. Zaidi, R. Baldemair, H. Tullberg *et al.*, "Waveform and numerology to support 5G services and requirements," *IEEE Commun. Mag*., vol. 54, no. 11, pp. 90–98, 2016.

[9] X. Zhang, L. Zhang, P. Xiao *et al.,* "Mixed numerologies interference analysis and inter-numerology interference cancellation for windowed OFDM systems," *IEEE Transactions on Vehicular Technology*, 2018.

[10] J. Sachs *et al*., "5G radio network design for ultra-reliable low-latency communication," *IEEE Network*, vol. 32, no. 2, pp. 24–31, 2018.

[11] A. Yazar, B. Pek¨oz, and H. Arslan, "Flexible multi-numerology systems for 5G new radio," *arXiv preprint*, arXiv:1805.02842, 2018.

[12] W. Timo *et al.*, "Mutual interference in OFDM-based spectrum pooling systems," in *Proc. 2004 IEEE 59th Vehicular Technology Conference. VTC 2004-Spring (IEEE Cat. No. 04CH37514)*, 2004, vol. 4, IEEE.

[13] P. Kumar and K. R. U. Rani, "Inter numerology interference reduction using windowing technique for OFDM based multi-numerologies," *Journal of Applied Science and Engineering*, vol. 26, no. 5, pp. 675–682, 2022.

[14] P. Kumar and K. R. U. Rani, "Inter numerology interference minimization using windowing and precoding techniques for 5G NOMA based OFDM numerologies," in *Proc. 2022 IEEE 2nd International Conference on Mobile Networks and Wireless Communications (ICMNWC)*, IEEE, 2022.

[15] X. Cheng, R. Zayani, H. Shaiek *et al*., "Inter-numerology interference analysis and cancellation for massive MIMO-OFDM downlink systems," *IEEE Access*, vol. 7, pp. 177164–177176, 2019.

[16] Y. Varun, K. S. Chandran *et al*., "Inter-numerology interference reduction based on precoding for multi-numerology OFDM systems," in *Proc. 2020 IEEE 3rd 5G World Forum (5GWF)*, IEEE, 2020.

[17] A. Goldsmith, S. A. Jafar, N. Jindal *et al*., "Capacity limits of MIMO channels," *IEEE Journal on Selected Areas in Communications*, vol. 21, no. 5, pp. 684–702, 2003.

[18] V. R. Cadambe and S. A. Jafar, "Interference alignment and degrees of freedom of the k-user interference channel," *IEEE Transactions on Information Theory*, vol. 54, no. 8, pp. 3425–3441, 2008.

[19] E. G. Larsson, O. Edfors, F. Tufvesson *et al*., "MassiveMIMO for next generation wireless systems," *IEEE Commun. Mag*., vol. 52, no. 2, pp. 186–195, Feb. 2014.

[20] L. Dai, B. Wang, Z. Ding *et al.*, "A survey of non-orthogonal multiple access for 5G," *IEEE Commun. Surveys Tuts*., vol. 20, no. 3, pp. 2294–2323, 3rd Quart., 2018.

[21] S. Sen, N. Santhapuri, R. R. Choudhury *et al*., "Successive interference cancellation: carving out MAC layer opportunities," *IEEE Transactions on Mobile Computing*, vol. 12, no. 2, pp. 346-357, Feb. 2013.

[22] A. Tasneem *et al.*, "Exact bit error-rate analysis of two-user NOMA using QAM with arbitrary modulation orders," *IEEE Communications Letters*, vol. 24, no. 12, pp. 2705–2709, 2020.

[23] I. Sharfer and A. O. Hero, "A maximum likelihood CDMA receiver using the EM algorithm and the discrete wavelet transform," in *Proc. 1996 IEEE International Conference on Acoustics, Speech, and Signal Processing Conference Proceedings*, pp. 2654–2657, vol. 5, 1996.

[24] Zhang, Xiaoying *et al*., "Mixed numerologies interference analysis and inter-numerology interference cancellation for windowed

OFDM systems," *IEEE Transactions on Vehicular Technology*, vol. 67, no. 8, pp. 7047–7061, 2018.

[25] New Radio - Physical Channels and Modulation (Release 15), *Document TS 38.211*, Version 15.1.0, 3GPP, Apr. 2018.

[26] I. T. Lu *et al*., "Combination of spectral and SVD precodings for out-of-band leakage suppression," in *Proc. 2013 IEEE Long Island Systems, Applications and Technology Conference (LISAT)*, IEEE, 2013.

[27] Q. W. He, Y. L. Hu, and A. Schmeink, "Closed-form symbol error rate expressions for non-orthogonal multiple access systems," *IEEE Transactions on Vehicular Technology*, vol. 68, no. 7, pp. 6775–6789, 2019.

[28] X. L. Wang, F. Labeau, and L. Mei, "Closed-form BER expressions of QPSK constellation for uplink non-orthogonal multiple access," *IEEE Communications Letters*, vol. 21, no. 10, 2017, pp. 2242–2245.